Invariant Multifractal Measures in Chaotic Hamiltonian Systems, and Related Structures

Martin C. Gutzwiller and Benoit B. Mandelbrot[a]
IBM T. J. Watson Research Center, Yorktown Heights, New York 10598
(Received 27 October 1987)

The coding of chaotic trajectories in Hamiltonian systems and the stochastic reflection of points on circles introduce examples of a new kind of multifractal measure, whose Hölder α ranges all the way from 0 to ∞.

PACS numbers: 05.45.+b, 03.20.+i, 46.10.+z

This Letter introduces and investigates some unusual multifractal measures on the real line which we have found independently, and for quite different reasons. Their salient feature is that $\alpha_{\min}=0$, and/or $\alpha_{\max}=\infty$, where α (in the notation of Mandelbrot,[1] p. 373, which is now widely accepted) is a Hölder exponent. These multifractal measures have the same general geometric origin, and we believe that they are the simplest representatives of a large class. One of us (M.C.G.) encountered his examples in classical Hamiltonian systems that display "hard chaos," while the other (B.B.M.) encountered his in what he calls "Fuchsian" or "Kleinian random flights," i.e., stochastic reflections of points on three or more circles, which may be cyclically tangent. Our first example, which is even simpler, involves elementary arithmetic; it originated in the third example, yet has turned out to be equivalent to the second. We will present our multifractals and their properties, and explain the underlying physics and the geometric motivation, mixing mechanics and geometry with arithmetic and analysis. Beyond the new examples of multifractal measure, the analysis provides a better understanding of the structure of phase space in Hamiltonian systems with hard chaos.

Our first and simplest arithmetic example represents a real number η by its continued fraction

$$n_0+\cfrac{1}{n_1+\cfrac{1}{n_2+\cdots}}.$$

To each $0<\eta<1$, i.e., when $n_0=0$ and $n_k\geq 1$ for $k>0$, the sequence n_k attaches the real number β (with $0<\beta<1$) whose binary expansion is made of n_1-1 times 0, followed by n_2 times 1, followed by n_3 times 0, and so on.

The functions $\beta(\eta)$ and $\eta(\beta)$ are continuous and monotone increasing. Since $\beta(1-\eta)=1-\beta(\eta)$, it suffices to represent $\beta(\eta)$ for $0\leq\beta\leq 0.5$ (Fig. 1). (The x and μ scales are explained in the second example.) However, the graph of $\beta(\eta)$ is not a devil's staircase, defined as the integral of a measure carried by a Cantor dust. In fact, $\beta(\eta)$ is singular and its derivative vanishes on an everywhere dense set, not in whole intervals. The bottom of the curve shows this feature quite clearly: Small values of η yield $n_1\simeq 1/\eta$, and therefore

$$\beta\simeq\exp(-n_1\ln 2)\simeq\exp[-(\ln 2)/\eta].$$

The same thing happens every time η gets close to a rational number, since there is then a large integer n_i in its continued fraction. Neither is the curve $\beta(\eta)$ the integral of the classic binomial measure (Ref. 1, p. 277), which refers to the set of points for which the digits 0 and 1 in binary representation have some specified limit frequencies q and $1-q$. Nevertheless, the increments of $\beta(\eta)$ define a multifractal measure.

For each interval $(\eta,\eta+\Delta\eta)$, one defines the Hölder α,

$$\alpha=\ln[\beta(\eta+\Delta\eta)-\beta(\eta)]/\ln\Delta\eta=\ln\Delta\beta/\ln\Delta\eta.$$

When the interval is chosen at random, the first descriptive characteristic of a multifractal is the distribution of the probability density of α. An important observation

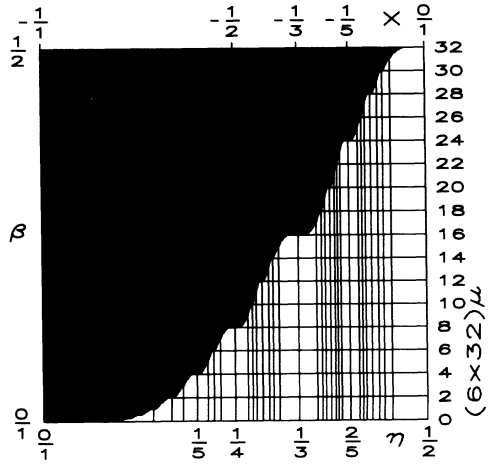

FIG. 1. A "slippery devil's staircase." This figure has two interpretations. The η and β scales concern the function $\beta(\eta)$ in the first example, computed for $0<\eta<\frac{1}{2}$. The abscissas of the vertical lines form the first levels of a Fairey series. The x and μ scales concern the function $\mu([-1,x])$ in the second example. This graph demonstrates the occurrence of very small values of the Hölder α.

by Frisch and Parisi[2] implies that the logarithm of this density is a fractal dimension. Recent papers describing applications of multifractals, beginning with the work of Halsey *et al.*,[3] denote this log(density) by $f(\alpha)$.

We have evaluated $f(\alpha)$ directly, from the numbers of occurrences of various $\Delta\beta=(\Delta\eta)^{\alpha}$ corresponding to a preselected $\Delta\eta$. The largest $\Delta\beta$ for a given $\Delta\eta$ was found to arise when η is the golden mean γ, and $\beta=\frac{2}{3}$. Thus $\alpha_{\min}=\ln 2/\ln(1/\gamma^2)=0.7202$, as confirmed numerically. The plot of $f(\alpha)$ has an extremely long tail as shown in Fig. 2. In fact, about 10% of the data are not plotted, because the $\Delta\beta$ were approximated by 0 in quadruple accuracy (precision of 112 bits $<10^{-33}$). For every rational η, one finds

$$\alpha=\lim_{\Delta\eta\to 0}\frac{\ln\Delta\beta}{\ln\Delta\eta}=\frac{(\ln 2)/\Delta\eta}{\ln\Delta\eta}=\infty.$$

The inverse curve $\eta(\beta)$ has very steep sections; its $f(\alpha)$ has the complementary shape: a long "head" in which $f(\alpha)$ is very close to α [observe that α is always an upper bound for $f(\alpha)$], and an ordinary short tail with $\alpha_{\max}=\ln(\gamma^{-2})/\ln 2=1.3885$, as confirmed numerically. Much larger samples were calculated; but double accuracy (8 bytes) is quite sufficient in this case; no $\Delta\eta$ are missing from Fig. 3.

Our second example in its simplest form involves the following three maps of the real line on itself: $x\to f_0(x)=1/x$, $x\to f_R(x)=2-x$, and $x\to f_L(x)=-2-x$. The square of each of these maps is the unit map. The group based on these three maps associates to every word w, i.e., to every ternary sequence of letters 0, R, and L, the product of a sequence of the maps f_0, f_R, and f_L. This group is the reduction to the real line of a bare-bones "Fuchsian group" whose fundamental domain is the singular triangle bounded by the circle of radius 1 centered at 0, and the vertical lines $x=1$ and $x=-1$. However, no knowledge of Fuchsian groups is required here, beyond the following two facts. (a) When the present group is extended to the complex plane by replacement of x by z, it has the whole real line as its limit set. That is, given the orbits z_0, under the actions of all the words w, the set of limit points of these orbits is the whole real line for every Z_0. (b) The group extended to the complex plane is continuous on the real line, and is discrete elsewhere. The orbit x_k of a real x_0 under the word w can return arbitrarily close to x_0 without returning exactly to x_0.

Now we move away from the Fuchsian background. We restrict the words so that two successive letters are different and the first letter is not 0 if $x\in[-1,1]$, is not L if $x<-1$, and is not R if $x>1$. Then each application of f_0 on an interval is contracting, and the application of f_R and f_L remain length preserving. Therefore, there exists an attractor that is independent of x_0, and hence only depends on the word w: It can be either of the points $x=1$, $x=-1$, and $x\pm\infty$; it can be a cycle of period ≥ 3 (if the word is periodic with the same period, after a finite number of arbitrary letters); it can be chaotic. Independently of x_0, the randomly chosen word w generates a random orbit, and the $x_k(w)$ form a sample from an underlying invariant measure, which is multifractal. This measure depends on the random process ruling w. Figures 4 and 5 show how this measure is distributed for a very long random word.

Let us describe the multifractal $\mu(dx)$ corresponding to symmetric binomial words, i.e., to words in which, given the previous letters, the two nonexcluded possibili-

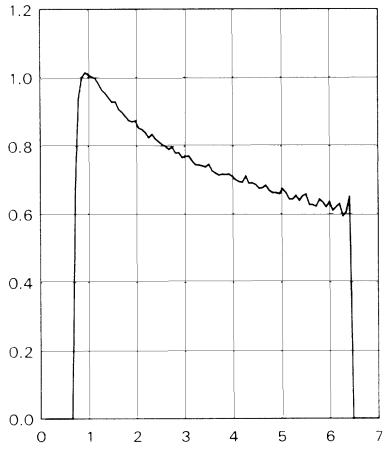

FIG. 2. The $f(\alpha)$ curve for the finite differences $\Delta\beta$, keeping $\Delta\eta=10^{-5}$. About 10% of the calculated $\Delta\beta$ are 0 in quadruple accuracy, i.e., $\Delta\beta<10^{-33}$ so that no data are available for $\alpha=\ln\Delta\beta/\ln\Delta\eta>6.5$; nevertheless the tail is infinitely long.

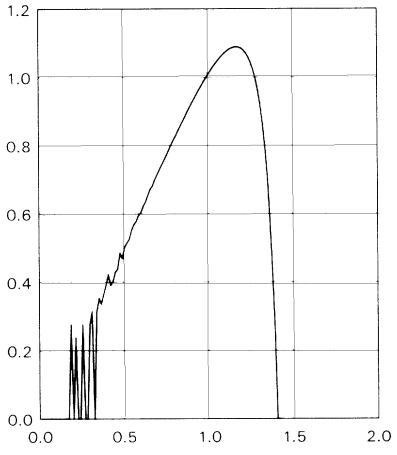

FIG. 3. The $f(\alpha)$ curve for the finite differences $\Delta\eta$ for constant values of $\Delta\beta=2^{-26}$. No data are missing; the curve starts linearly with slope 1, indicating very small values of α. This linear dependence for $\alpha<1$ is obscured because very few data are available for small α. The largest jumps in η occur at $\beta=0$ and 1, where $\Delta\eta=\frac{1}{26}$, so that $\alpha=\ln\Delta\eta/\ln\Delta\beta\geq\ln 26/26\ln 2=0.1786$, as is indeed observed.

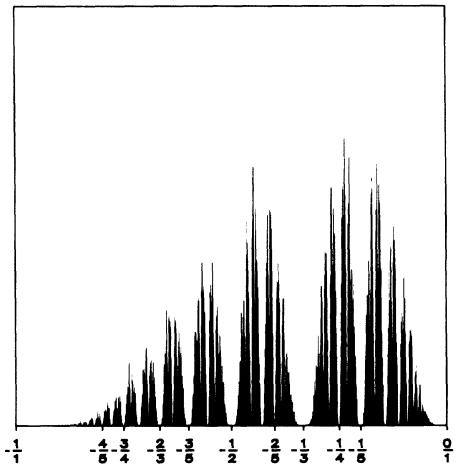

FIG. 4. Sample measures of small intervals of x for the symmetric binomial multifractal measure defined by inversion in three circles. Plotted for $-1<x<0$.

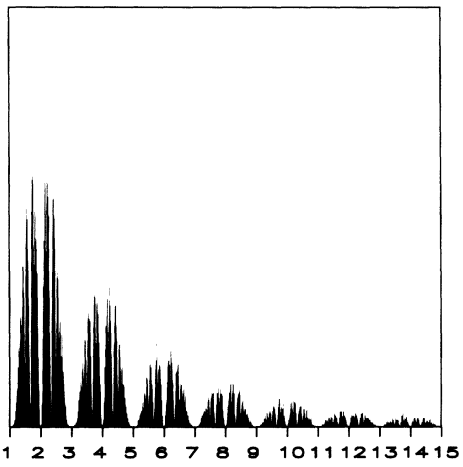

FIG. 5. Same as Fig. 4, but for $1<x<15$.

ties for the next letter both have the probability $\frac{1}{2}$. We shall show that for $0<x<1$, $\mu([-1,x])=\frac{1}{3}\beta(\frac{1}{2}+\frac{1}{2}x)$, where $\beta(\eta)$ is the function in the first example. This explains the scales to the bottom and to the right of Fig. 1.

By obvious symmetries $\mu([-\infty,-1])=\mu([-1,1])=\mu([1,\infty])=\frac{1}{3}$, and the distribution of μ is expressed most compactly in terms of $\beta(\eta)$. The rule is that if $\eta(p2^{-k})=n'/d'$ and $\eta((p+1)2^{-k})=n''/d''$ with p, k, n', n'', d', and d'' integers >0, one has $\eta((p+\frac{1}{2})2^{-k})=(n'+n'')/(d'+d'')$. This is the Fairey subdivision.

It is easy to expand to asymmetric binomial words and to letter sequences ruled by Markov processes, or by other processes without long memory.

Our third example starts with the singular quadrangle D_2 in the upper (x,y) plane whose boundaries are the two circles of radius $\frac{1}{2}$ centered on $x=-\frac{1}{2}$ and on $x=+\frac{1}{2}$, and the vertical lines $x=-1$ and $x=+1$. A torus is obtained if one identifies the opposite sides. This torus has one exceptional point, however, because the vertex of the quadrangle is infinitely far away in the metric $ds^2=(dx^2+dy^2)/y^2$ of the hyperbolic plane. (One can think of the torus as a closed box, and of the exceptional point as a narrow opening for the particle to enter and to exit, as if it were scattered from some molecule with an internal degree of freedom.)[4]

The next step is inspired by the work of Series.[5] She considers a singular triangle D_1, the right-hand half of D_2, which is bounded by the circle of radius $\frac{1}{2}$ centered in $x=\frac{1}{2}$, and by the vertical lines $x=0$ and $x=1$. A geodesic is represented by a Euclidean circle, centered on the x axis, which goes from $x=\xi$ (past) to $x=\eta$ (future). Consider the special case $\xi<0<\eta$; the geodesic enters D_1 through the vertical side $x=0$. If $0<\eta<1$, the geodesic leaves D_1 through the circle and is brought back into D_1 by the transformation $z'=z/(1-z)$. If $1<\eta<\infty$, the geodesic leaves D_1 through the vertical $x=1$ and is brought back into D_1 by $z'=z-1$. In the first case, the geodesic is said to turn right, while in the second case, it makes a left turn.

If one continues in this manner the future of the geodesic is associated with a sequence of letters R and L, or equivalently with a sequence of integers $(n_0,n_1,n_2,\ldots)$ which indicates n_0 times L, followed by n_1 times R, followed by n_2 times L, and so on. The sequence of letters is best represented by a real β with the same binary expansion, while, most remarkably,

$$\eta=n_0+\cfrac{1}{n_1+\cfrac{1}{n_2+\cfrac{1}{\cdots}}}.$$

Therefore, the functions $\beta(\eta)$ and $\eta(\beta)$ at the beginning of this Letter connect the intuitive description of the geodesic β and its coordinate with respect to the singular triangle η.

Functions with the same unusual characteristics appear in the singular quadrangle D_2 and can be interpreted as physical properties of chaotic Hamiltonian systems. The starting point ξ and the end point η of a geodesic can be used as coordinates in a Poincaré surface of section with the invariant element of area $d\xi\,d\eta/(\xi-\eta)^2$. The four sides of the quadrangle correspond to the intervals $\{1\}=(-\infty,1)$, $\{2\}=(-1,0)$, $\{3\}=(0,1)$, and $\{4\}=(1,\infty)$ on the x axis. Entry and exit of the geodesic are determined by the intervals to which ξ and η belong.

Opposite sides of D_2 are mapped into one another by $z\rightarrow z'=(az+b)/(cz+d)$, written as $(a,b;c,d)$ in flattened notation, where a,b,c,d are real and $ad-bc=1$. Side $\{1\}$, the vertical $x=-1$, is mapped into $\{3\}$, the circle around $x=\frac{1}{2}$, by $A=[\delta,\delta;\delta,(1+\delta^2)/\delta]$; side $\{4\}$, the

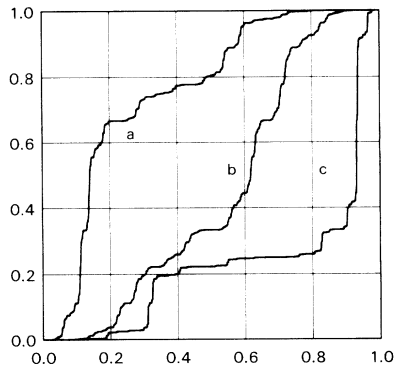

FIG. 6. The functions $\theta(\eta)$ for $\delta=1/\sqrt{7}$ (curve a), 1 (curve b), and $\sqrt{7}$ (curve c) have the same properties as $\beta(\eta)$; each portrays the relations between two invariant measures on the Poincaré surface.

vertical $x=1$, is mapped into $\{2\}$, the circle around $x=-\frac{1}{2}$, by $B=[\delta,-\delta;-\delta,(1+\delta^2)/\delta]$. The parameter $\delta>0$ describes a family of nonequivalent geometries on D_2. A further parameter γ could be introduced, but would require a less symmetric singular quadrangle than D_2.

The "story" of a trajectory in D_2 is told by the sequence of sides it crosses. This story is encoded in a word with an alphabet of three letters, $R(=\text{right}=0)$, $S(=\text{straight}=1)$, and $L(=\text{left}=2)$ in the obvious manner: following $\{1\}$, side $\{2\}$ is right, $\{3\}$ is straight, and $\{4\}$ is left; etc. The computation for the future sequence depends only on η, while the past sequence depends only on ξ. Thus, a function from $0<\eta<1$ to $0<\theta<1$ is defined where the ternary expansion of θ gives the story of the trajectory. Figure 6 shows $\theta(\eta)$ for the three values $\delta=1/\sqrt{7}$, $\delta=1$, and $\delta=\sqrt{7}$.

The multifractal analysis of $\theta(\eta)$ gives results like $\beta(\eta)$. The infinitely long tail in the $f(\alpha)$ curve is now due to the existence of parabolic elements in the group which is generated by A and B; e.g., the sequence 0000 leads to $BAB^{-1}A^{-1}=(-1,0;\Gamma,-1)$ with $\Gamma=2(2+\delta^{-2})$. A simple argument then shows that $\theta(\eta)$ starts with $\theta\cong\exp(-\Gamma\ln 3/4\eta)$.

The presence of almost flat pieces in the graph of $\theta(\eta)$ indicates that the trajectory gets trapped in the exit-entry, as opposed to wandering around the torus, i.e., interacting with the internal degree of freedom. Thus, θ gives the physically more informative description than η; but both define invariant measures on the Poincaré surface of section; they can be reduced to the one-dimensional $\theta(\eta)$ curve because past and future are decoupled. The $f(\alpha)$ curve characterizes the chaos in this system, because it relates the coding of the trajectories to their physical parameters (initial conditions). This connection is important in the sum over all trajectories (classical approximation to Feynman's path integral), or in the sum over all periodic orbits as in Selberg's trace formula. As shown by Gutzwiller[6] for the anisotropic Kepler problem where the coding is binary, such sums can be computed explicitly as sums over code words.

Several of the figures were prepared by Rejean Gagné.

[a]Also at Yale University, New Haven, CT 06520.

[1]B. B. Mandelbrot, *The Fractal Geometry of Nature* (Freeman, New York, 1982).

[2]U. Frisch and G. Parisi, in *Turbulence and Predictability in Geophysical Fluid Dynamics and Climate Dynamics,* International School of Physics "Enrico Fermi," Course 88, edited by M. Ghil *et al.* (North-Holland, Amsterdam, 1985), pp. 84–88.

[3]T. C. Halsey, M. H. Jensen, L. P. Kadanoff, I. Procaccia, and P. E. Shraiman, Phys. Rev. A **33**, 1141 (1986).

[4]M. C. Gutzwiller, Physica (Amsterdam) **7D**, 341 (1983).

[5]C. Series, J. London Math. Soc. (2) **31**, 69 (1985), and Ergodic Theory Dynamical Systems **6**, 601 (1986). A geometric interpretation is found in Math. Intelligencer **7**, 20 (1985).

[6]M. C. Gutzwiller, Phys. Rev. Lett. **45**, 150 (1980).